Piezoresistive transduction in multilayer polycrystalline silicon resonators

J. D. Cross,[1,a)] B. R. Ilic,[1] M. K. Zalalutdinov,[2,3] W. Zhou,[1] J. W. Baldwin,[3] B. H. Houston,[3] H. G. Craighead,[1] and J. M. Parpia[1]
[1]*Cornell University, Ithaca, New York 14853, USA*
[2]*Global Strategies Group, Crofton, Maryland 21114, USA*
[3]*Naval Research Laboratory, Washington, DC 20375, USA*

(Received 11 June 2009; accepted 9 September 2009; published online 1 October 2009)

We demonstrate piezoresistive transduction of mechanical motion from out-of-plane flexural micromechanical resonators made from stacked thin films. The resonators are fabricated from two highly doped polycrystalline silicon layers separated by an interlayer dielectric. We examine two interlayer materials: thermal silicon dioxide and stoichiometric silicon nitride. We show that via one-time dielectric breakdown, the film stack functions as a vertical piezoresistor effectively transducing the motion of the resonators. We obtain a gauge factor of ~5, which is sufficient to detect the resonator motion. The simple film stack constitutes a vertically oriented piezoresistor that is readily integrated with micro- and nanoscale resonators. © *2009 American Institute of Physics*. [doi:10.1063/1.3241077]

One of the challenges of implementing microelectromechanical structures (MEMS) or nanoelectromechanical structures (NEMS) in applications such as sensors or frequency determining communications elements is signal transduction from the resonant structure.[1–8] This problem is increasingly severe as device sizes are scaled down to the sub-micron regime making capacitive coupling difficult and resulting in a drastic impedance mismatch between the mechanical device and conventional 50 Ω electronics.[3,4,9,10]

Various approaches that attempt to address these MEMS and NEMS electrical integration challenges include: frequency conversion,[2] piezoresistive strategies,[3,10,11] or impedance matching circuitry.[4] We report on a structural approach to the electrical transduction problem. We describe a vertically oriented piezoresistive transducer across multiple thin film layers. The structure is inspired by layers present in double-polycrystalline silicon complementary metal-oxide-semiconductor (CMOS) foundry processes,[6] and as such, is amenable to integration with minimal process disruption. A further advantage of this approach is that the piezoresistive transducer is integral to the resonator—there is no need to add thin metal films or perform ion implantation. This method is only limited by the lithography used to create the resonators and the properties and thickness of the interlayer dielectric.

All experiments are performed on a test structure comprised of six "in series" bridges shown in Fig. 1, operated in a vacuum chamber at pressures below 1 Torr (typically 100–500 mTorr). The optical detection and thermoelastic drive setup used for these experiments has been described elsewhere.[1] Electrical connections are made to gold bond pads contacting the top and bottom polycrystalline silicon layers (Fig. 1 inset). The MEMS chip is wirebonded to a 24-pin dual in-line package mounted in a vacuum chamber so that electrical connections to the chip and optical observations of the chip can be made simultaneously.

Two film stacks were used to create the devices; one consists of low-pressure chemical vapor deposition (LPCVD) polycrystalline silicon atop thermal silicon dioxide atop LPCVD polycrystalline silicon (p-sox-p), and the other is LPCVD polycrystalline silicon atop LPCVD silicon nitride atop LPCVD polycrystalline silicon (p-sn-p). Both stacks sit atop sacrificial silicon dioxide and a silicon handle wafer (Fig. 1 inset).

Initially, we use optical methods to evaluate the mechanical properties of the resonators. For both stacks we observe a range of quality factors (Q) from around 300 to a few thousand. For single layer polycrystalline silicon devices, we generally observe Q in the thousands to tens of thousands.

Figure 2(a) shows how ac and dc connections are made to the top and bottom polycrystalline silicon layers. Depending upon the particular experiment, not all connections are necessary. Typically, both electrical and optical experiments are performed with dc voltages applied on both the top and bottom layers, though one of the dc voltages may be set to 0 V.

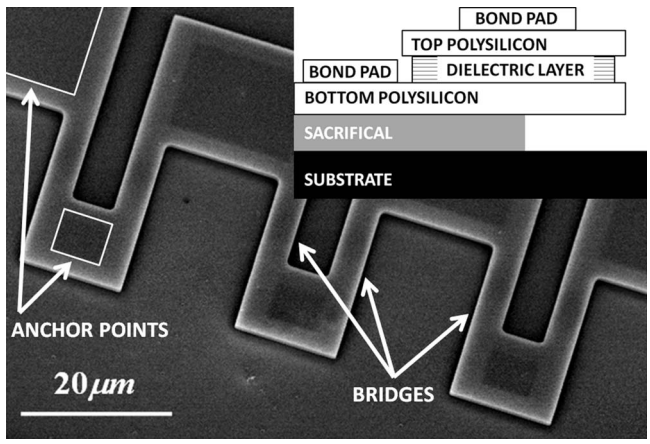

FIG. 1. A scanning electron micrograph showing the six-bridge structure common to p-sox-p and p-sn-p devices (image is of p-sox-p device). Layer thicknesses are: (p_{bottom}-sox-p_{top}) 277 nm-53 nm-303 nm; (p_{bottom}-sn-p_{top}) 280 nm-50 nm-106 nm. Contrast is altered to highlight the undercut at the anchor points, which are highlighted in white as are three of the six bridges. The gold bond pads are not shown. Inset: a side-view schematic of the layer stack.

a)Electronic mail: jdc47@cornell.edu.

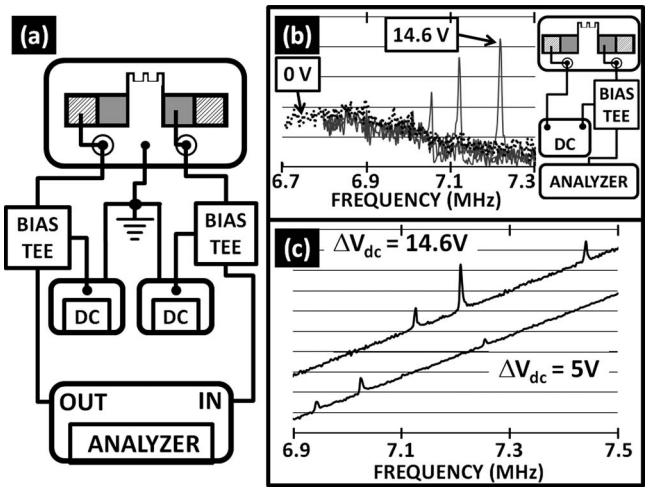

FIG. 2. (a) Schematic showing how the p-sox-p resonators are driven or detected with dc bias and ac input or output on two different ports. (b) Data from optically driven and electrically detected resonators. The substrate is grounded, and the bottom and top polycrystalline silicon layers have dc connections. The top polycrystalline silicon layer is connected to the input of the analyzer. The four curves show increasing voltage difference between the layers, from 0 V (dotted black) to 7, 11, and 14.6 V. The increase in the resonance frequency of the device is commonly observed and results from electrostatic displacement due to capacitive coupling. (c) Results from electrically driving and detecting the resonators. Three of six peaks are shown, from three of the six total resonators. Both layers have dc bias connections, and the bottom layer is driven by the output of the analyzer, while the top layer is connected to the input of the analyzer. Both frequency and amplitude are seen to shift when the voltage difference between the layers is changed (the substrate is grounded).

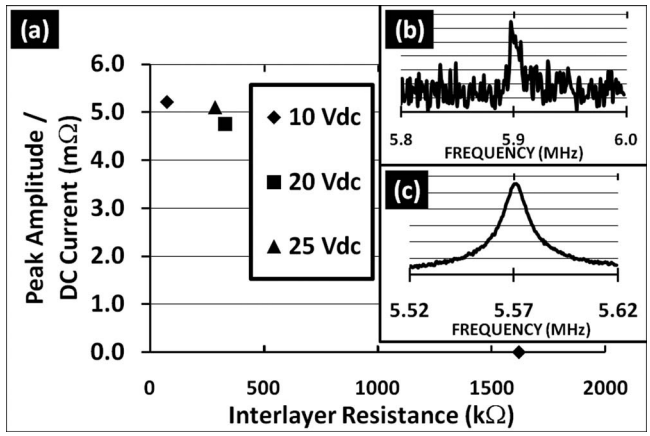

FIG. 3. (a) Peak detected amplitude divided by dc current for p-sn-p devices as a function of interlayer resistance. Data is from optical drive and electrical detection experiments (see (b)). (b) Data from an optical drive and electrical detection experiment using p-sn-p devices. The peak amplitude from experiments similar to (b) is compiled in the graph in (a). (c) Optical drive and optical detection of a p-sn-p resonator. The curve in (c) demonstrates a linear response of the resonator, while the curve in (b) is nonlinear. It has been necessary to drive the p-sn-p devices nonlinearly to detect any signal electrically.

Figure 2(b) shows the results of an optical (thermoelastic) drive[1] and electrical detection experiment on a p-sox-p device. The top polycrystalline silicon layer is connected to a dc bias power supply and the input of the network analyzer. The bottom polycrystalline silicon layer is connected only to a dc power supply. As the potential difference is increased between the two layers, the detected signal strength and frequency increase in amplitude. Reversing the top and bottom layer potentials produces similar results, and no signal is observed with the potential difference is 0 V, nor when one layer is floating relative to ground.

The resonators can also be driven and detected electrically [Fig. 2(c); three of six peaks from three of six resonators are shown in the spectra]. Electrical drive is a combination of capacitive coupling with the substrate and thermoelastic due to the dc current between polycrystalline silicon layers. No amplifier is used to enhance the detected signal; neither is there any impedance matching circuitry, nor any frequency up- or down-mixing. The sloping background signal is the result of electrical cross-talk between polycrystalline silicon layers.

We measure the interlayer resistance (top to bottom polycrystalline silicon) to be on the order of 10^4 kΩ up to a few megaohms for most of the p-sox-p devices tested. From any starting value, the interlayer resistance can be decreased to $\sim 10^4$ kΩ by a one-time application of interlayer voltages above a breakdown threshold of about 30 V for most p-sox-p devices.

All experiments have also been performed using identical geometry resonators with intermediate layer silicon nitride. The p-sn-p devices are investigated to confirm that any undercut or damage to the interlayer silicon dioxide of the p-sox-p devices is not the primary cause of the transduction mechanism. Figure 3(a) shows the results of a series of experiments on a single p-sn-p device. Data are the peak amplitude at resonance (electrical detection and optical drive) divided by the static current. The interlayer resistance is broken down by one-time applications of increasingly higher voltage differences across the polycrystalline silicon layers. Up to a 35 V difference is used to decrease the resistance from an initial value of 1.6 MΩ down to a final value of 74 kΩ. At 330 kΩ and below we observe an electrical signal from the displacement of the resonators at their resonant frequency.

An example of a peak used to generate the data for Fig. 3(a) is shown in Fig. 3(b). With p-sn-p devices, electrical signals are only detectable when the devices are driven in the nonlinear regime. The transduction is apparently less effective for the p-sn-p devices than for the p-sox-p devices, which all exhibit stronger electrical peaks even in the linear regime. Figure 3(c) shows a p-sn-p device driven (linearly) and detected optically.

We estimate the gauge factor for the p-sox-p material by assuming that the piezoresistance arises from the geometric effect of squeezing and deforming the intermediate layer during out-of-plane motion of the resonator. We disregard the possible contribution to the gauge factor from the fractional change in resistivity, and arrive at a gauge factor of[10,12,13]

$$\frac{dR}{R}\Big/\frac{dh}{h} = \frac{dR}{R}\Big/\left(\sigma\frac{dL}{L}\right) = \gamma, \tag{1}$$

where R is the resistance, h is the thickness of the entire film stack, L is the length of the double-clamped beam, and $\sigma \sim 0.2$ is the Poisson ratio for the material (thermal silicon dioxide).[14] In our configuration $dR/R = V_{\mathrm{ac}}^{\mathrm{measured}}/\Delta V_{\mathrm{dc}}^{\mathrm{top\text{-}bottom}}$, which is directly measured. dL/L is calculated from the critical amplitude at which nonlinear motion occurs. A signal at the resonance frequency is observed because the polycrystalline silicon layers are not the same thickness. We obtain data on the transition from linear to nonlinear motion to relate the detected voltage to the critical amplitude of motion.[15–17] For

one device tested, the onset of nonlinear motion begins at an ac drive amplitude between layers of about 40 mV (dc voltage between layers is 24.4 V). The critical amplitude for this device is ~8 nm, and the detected voltage of the nonlinear peak is 40 μV. From these values, the gauge factor is estimated to be ~5, and is certainly adequate to directly detect the motion of the resonators without the need for amplification, signal mixing, or impedance matching. This value compares favorably with other reported gauge factors for piezoresistive materials used to detect resonator motion.[3,5,10,11,13,18,19]

We have fabricated and tested multilayer resonators consisting of top-and bottom-layer polycrystalline silicon films with an intermediate insulating layer and shown that out-of-plane vibration of these devices can be detected electrically, whether driven electrically or optically. The piezoresistive transduction mechanism is vertically oriented through the film stack. The transduction is shown to be adequate for directly electrically detecting the resonant motion of the devices without the need for impedance matching circuitry or signal amplification. Furthermore, the transduction mechanism is indistinct from the resonator itself, so problems associated with scaling down device sizes are potentially avoided. This also greatly reduces the effort associated with fabricating a displacement transducer and affords the possibility of optimizing the transducer (via the intermediate layer) for particular applications. Finally, we note that the p-sox-p film stack is readily available in any multilayer polycrystalline silicon CMOS foundry processes, opening up the possibility of directly integrating MEMS devices and transducers with CMOS.

This research was supported at Cornell University by DARPA (Contract No. HR0011-06-1-0042) and at the Naval Research Laboratory by the Office of Naval Research. Fabrication was performed at the Cornell Nanoscale Science and Technology Facility, and certain measurements were performed at the Cornell Center for Nanoscale Systems.

[1] D. W. Carr, L. Sekaric, and H. G. Craighead, J. Vac. Sci. Technol. B **16**, 3821 (1998).
[2] I. Bargatin, E. B. Myers, J. Arlett, B. Gudlewski, and M. L. Roukes, Appl. Phys. Lett. **86**, 133109 (2005).
[3] R. B. Reichenbach, M. Zalalutdinov, J. M. Parpia, and H. G. Craighead, IEEE Electron Device Lett. **27**, 805 (2006).
[4] P. A. Truitt, J. B. Hertzberg, C. C. Huang, K. L. Ekinci, and K. C. Schwab, Nano Lett. **7**, 120 (2007).
[5] R.J. Wilfinger, P.H. Bardell, and D.S. Chhabra, IBM J. Res. Dev. **12**, 113 (1968).
[6] M. Villarroya, J. Verd, J. Teva, G. Abadal, E. Forsen, F. P. Murano, A. Uranga, E. Figueras, J. Montserrat, J. Esteve, A. Boisen, and N. Barniol, Sens. Actuators, A **132**, 154 (2006).
[7] S. Evoy, D. W. Carr, L. Sekaric, A. Olkhovets, J. M. Parpia, and H. G. Craighead, J. Appl. Phys. **86**, 6072 (1999).
[8] L. Sekaric, M. Zalalutdinov, S. W. Turner, A. T. Zehnder, J. M. Parpia, and H. G. Craighead, Appl. Phys. Lett. **80**, 3617 (2002).
[9] Y. Xie, S.-S. Li, Y.-W. Lin, Z. Ren, and C. T.-C. Nguyen IEEE Trans. Ultrason. Ferroelectr. Freq. Control **55**, 890 (2008).
[10] M. Li, H. X. Tang, and M. L. Roukes, Nat. Nanotechnol. **2**, 114 (2007).
[11] V. Mosser, J. Suski, J. Goss, and E. Obermeier, Sens. Actuators, A **28**, 113 (1991).
[12] R. L. Parker and A. Krinsky, J. Appl. Phys. **34**, 2700 (1963).
[13] J. A. Harley and T. W. Kenny, Appl. Phys. Lett. **75**, 289 (1999).
[14] M. T. Kim, Thin Solid Films **283**, 12 (1996).
[15] H. W. Ch. Postma, I. Kozinsky, A. Husain, and M. L. Roukes, Appl. Phys. Lett. **86**, 223105 (2005).
[16] A. H. Neyfeh and D. T. Mook, *Nonlinear Oscillations* (Wiley, New York, 1979), pp. 161–175.
[17] W. Weaver, Jr., S. P. Timoshenko, and D. H. Young, *Vibration Problems in Engineering*, 5th ed. (Wiley, New York, 1990), pp. 166–175.
[18] R. He, X. L. Feng, M. L. Roukes, and P. Yang, Nano Lett. **8**, 1756 (2008).
[19] J. L. Arlett, J. R. Maloney, B. Gudlewski, M. Muluneh, and M. L. Roukes, Nano Lett. **6**, 1000 (2006).